Chemical Science

ROYAL SOCIETY OF CHEMISTRY

EDGE ARTICLE

View Article Online
View Journal | View Issue

Cite this: *Chem. Sci.*, 2024, **15**, 1283

All publication charges for this article have been paid for by the Royal Society of Chemistry

Enhancing NIR-to-visible upconversion in a rigidly coupled tetracene dimer: approaching statistical limits for triplet–triplet annihilation using intramolecular multiexciton states†

Alexander T. Gilligan,‡[a] Raythe Owens,‡[a] Ethan G. Miller,[a] Nicholas F. Pompetti[a] and Niels H. Damrauer *[ab]

Important applications of photon upconversion through triplet–triplet annihilation require conversion of near-IR photons to visible light. Generally, however, efficiencies in this spectral region lag behind bluer analogues. Herein we consider potential benefits from a conformationally well-defined covalent dimer annihilator TIPS-BTX in studies that systematically compare function to a related monomer model TIPS-tetracene (TIPS-Tc). TIPS-BTX exhibits weak electronic coupling between chromophores juxtaposed about a polycyclic bridge. We report an upconversion yield ϕ_{UC} for TIPS-BTX that is more than 20× larger than TIPS-Tc under comparable conditions (0.16%). While the dimer ϕ_{UC} is low compared to bluer champion systems, this yield is amongst the largest so-far reported for a tetracenic dimer system and is achieved under unoptimized conditions suggesting a significantly higher ceiling. Further investigation shows the ϕ_{UC} enhancement for the dimer is due exclusively to the TTA process with an effective yield more that 30× larger for TIPS-BTX compared to TIPS-Tc. The ϕ_{TTA} enhancement for TIPS-BTX relative to TIPS-Tc is indicative of participation by intramolecular multiexciton states with evidence presented in spin statistical arguments that the ^{5}TT is involved in productive channels. For TIPS-BTX we report a spin-statistical factor $f = 0.42$ that matches or exceeds values found in champion annihilator systems such as DPA. At the same time, the poor relative efficiency of TIPS-Tc suggests involvement of non-productive bimolecular channels and excimeric states are suspected. Broadly these studies indicate that funneling of photogenerated electronic states into productive pathways, and avoiding parasitic ones, remains central to the development of champion upconversion systems.

Received 11th September 2023
Accepted 11th December 2023

DOI: 10.1039/d3sc04795d

rsc.li/chemical-science

Introduction

Generation of anti-stokes shifted electronic states relative to their excitation source and their application towards driving photophysical processes is an area of interest for both fundamental science and a blossoming scope of applications including solar energy conversion,[1–7] photoredox catalysis,[8–11] bioimaging and therapies,[12–16] and 3D printing[17,18] to name a few. One method of anti-stokes generation heralded for its promise in low excitation intensity scenarios is triplet–triplet annihilation upconversion (TTA-UC).[2,19–24] TTA-UC generally comprises a system of molecules where one species with a low energy singlet (S_1) state, referred to as the sensitizer (Sen), is first photoexcited and efficiently undergoes intersystem crossing into its triplet (T_1) state. This is often driven by the heavy atom effect, for example in the palladium phthalocyanine species used here. Following collision in solution-phase diffusional systems that are common, the energy is transferred to the T_1 of a harvesting molecule, referred to as the annihilator (An). Finally, collisions between two excited triplet annihilators (homofusion) or between a triplet sensitizer and a triplet annihilator (heterofusion) lead to the generation of an annihilator S_1 that can fluoresce with photon energy greater than the excitation source (see Scheme 1). The conversion is mediated by an intermolecular multiexciton state and potentially other higher excited states within the collisional partners.

While upconversion has been studied with many molecular partners, a prototypical champion system in solution to be emulated consists of the annihilator 9,10-diphenylanthracene (DPA) and a metal porphyrin species (Zn, Pd or Pt octaethylporphyrin for example). Indeed, a growing body of literature on DPA has reported upconversion quantum yields ϕ_{UC} of order ~25%.[25,26] However, usage of DPA restricts upconversion

[a]*Department of Chemistry, University of Colorado Boulder, Boulder, Colorado 80309, USA. E-mail: niels.damrauer@colorado.edu*

[b]*Renewable and Sustainable Energy Institute (RASEI), University of Colorado Boulder, Boulder, Colorado 80309, USA*

† Electronic supplementary information (ESI) available. See DOI: https://doi.org/10.1039/d3sc04795d

‡ These authors contributed equally to this work.

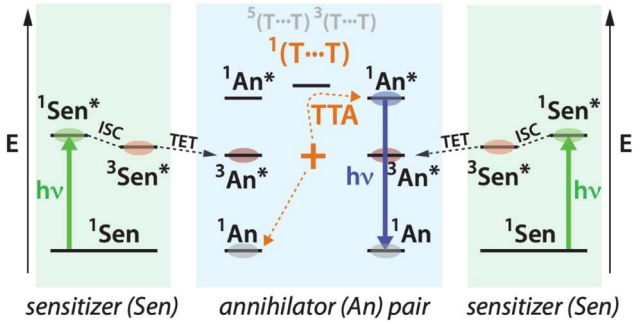

Scheme 1 Representation of TTA-UC with relevant states and processes central to determination of upconversion yield ϕ_{UC}. The intermolecular multiexciton singlet is shown as mediating the TTA event but other excited states can also be involved.

photoluminescence to the blue region of the visible spectrum and excitation must be in the green at ~520 nm. For many applications these restrictions are prohibitive. For example, with photovoltaics upconversion would be valuable by way of harvesting sub-bandgap photons. The green visible spectrum is not useful for current solar-cell technologies of importance, ranging from organic to perovskite to crystalline silicon devices.[4] For bioimaging and 3D printing, higher photon energy excitation sources run into issues of scattering and tissue penetration.[27,28] It would therefore be beneficial if upconversion could move to redder emitting annihilators and excitation sources in so-called NIR-to-visible upconversion, a field that has recently been reviewed.[23]

A natural path forward for lowering S_1 is to employ larger acenes such as substituted tetracenic species. This is approximately the limit in acene size before singlet fission – which is more exoergic in pentacenic materials[29] – begins to significantly undermine TTA. Rubrene (5,6,11,12-tetraphenyltetracene) has been extensively explored due to its near-unity fluorescence quantum yield and shows a red-shifted peak emission compared to DPA, for example at ~560 nm in room temperature toluene.[30–33] Here we focus on solution phase upconversion systems rather than films that incorporate rubrene.[34–41] An earlier (2010) exploration of TTA-UC for rubrene in solution analyzed statistical factors tied to the photophysical outcome of different spin channels in the triplet–triplet encounter complex (commonly referred to as *f*, *vide infra*).[31] They reported favorable properties, exceeding ones seen for DPA, suggesting that a sizable amount of the spin-triplet encounter complex population is able to dissociate without individual triplet loss, in the same way as the spin-quintet encounter complexes. However, upconversion yields for rubrene in solution, even in optimized TTA-UC systems, are muted relative to DPA with values lower than a factor of five, often significantly so.[23,30,32,42–46] More recent experiments on rubrene exploring the same spin statistics while using lower excitation peak intensities question the 2010 results and suggest they are skewed by measurement conditions.[32] These authors see a statistical factor *f* at 15%[32] that is a factor of four smaller than the earlier report (60%),[31] and only modestly larger than expected if only the spin-singlet encounter complex channel is productive while the spin-triplet and spin-quintet encounter complexes decay fully to ground state (11.1%; *i.e.*, $f = \frac{1}{9}$). They suggest this lies at the heart of the less than ideal ϕ_{UC} properties for rubrene. It is noted that in terms of ϕ_{UC}, other tetracenic systems such as BPEN (5,12-bis(phenylethynyl)naphthacene),[16] or TIPS-tetracene (*vide infra* and ref. 33, 47 and 48) do not fare better. Whether or not there is a common origin of poor performance in the statistical factor is to be determined, but it is clear that new strategies aimed to improve the upconversion limits of larger acenes would be valuable.

We and others have considered potential benefits within dimers and oligomers comprising covalently fused annihilators.[26,33,47,49–57] In principle, intramolecular multiexciton states in such systems could participate in excited state dynamics, perhaps in productive ways.[33] From a technological perspective dimers and oligomers are also interesting in settings where one cannot rely on diffusion to bring pairs of triplet annihilator species together, for example at nanomaterial/molecular interfaces where the nanomaterial functions as a triplet sensitizer to the bound species. For dimers derived from anthracenic chromophores, studied in common diffusive solution phase experiments with a molecular sensitizer, there is not yet evidence for advantage derived from intramolecular multiexciton states.[26,51] In these systems there is a strong energetic driving force for annihilation ($E_{S_1} < E_{T_1} + E_{T_1}$), and it appears that intermolecular encounter complexes provide sufficiently productive excited-state precursors. This does not mean that such systems will not be valuable in non-diffusive settings, only that they do not yet provide evidence for the relevance of intramolecular multiexciton states in mediating productive dynamics.

As a point of contrast, there is growing evidence that tetracenic dimers may behave differently, potentially offering opportunities to improve redder emitting platforms. There are now several reports showing benefits of covalently fused systems over monomer models, although these studies have not all specifically quantified TTA yields or use the same definitions for ϕ_{UC}, so direct comparisons are challenging. Wilson and coworkers in collaboration with members of our group considered a rigid norbornyl-bridged TIPS-tetracene dimer called TIPS-BT1′ compared to the monomer models TIPS-tetracene (TIPS-Tc) and rubrene and found upconversion brightness to be higher in the dimer at comparable annihilator concentrations.[33] This work also found advantage for the dimer at comparable triplet flux, which is a surrogate for relative TTA yield. Congreve, Campos, and coworkers studied a series of non-rigid TIPS-tetracene dimers linked at chromophore end positions by varying *p*-phenylene spacers ($n = 0$, 1, 2, and 4).[47] In two of their dimer systems ($n = 1$ and 2), they also found that upconversion brightness is larger than TIPS-Tc at comparable annihilator concentrations. At the highest concentration considered, the $n = 1$ and $n = 2$ dimers are brighter TTA-UC emitters than TIPS-Tc by a factor of approximately 4 and 2, respectively. Finally, Guldi, Tykwinski, and coworkers recently explored two non-rigid tetracene dimer types with either a meta-substituted diethynylphenylene bridge or a 1,3-

diethynyladamantyl bridge relative to monomer models with bridge-specific substituents.[56] They also found that the dimers are brighter TTA-UC emitters compared to the respective monomer models at comparable annihilator concentrations, with relative ratios of approximately 4 and 3 for the phenylene and adamantyl comparisons, respectively. They have also considered upconversion yields ϕ_{UC}, as we do here, and at the highest annihilator concentrations they consider, found ratios of 3.7 and 2.8 favoring the dimers for the phenylene and adamantyl comparisons, respectively. In the current work, we consider the behavior of another rigid dimer system, this time utilizing a larger fused polycyclic bridge comprising both saturated and unsaturated fragments constructed using Pd-catalyzed annulation chemistry.[58,59] We measure upconversion yields and disentangle them into yields of contributing photophysical processes with an eye towards enabling direct comparisons between dimer *versus* monomer. The results suggest significant advantages for the dimer including a ~20× enhancement of ϕ_{UC} and a ~35× enhancement of ϕ_{TTA} relative to TIPS-Tc at comparable concentrations. These studies provide evidence that intramolecular multiexciton states play decisive roles controlling upconversion yield in these NIR-visible TTA-UC systems.

Results and discussion

Annihilator properties

As described in the Introduction, this work seeks to compare TTA-UC properties of the monomer model TIPS-Tc relative to a new rigid dimer system TIPS-BTX that utilizes the same acene chromophore (see stick structures for both in Fig. 1). The synthesis of TIPS-BTX and the isolation of the syn-diastereomer were reported elsewhere,[58,59] but briefly, it is prepared through a palladium-catalyzed arene-norbornene annulation reaction (CANAL) that generates the two cyclobutene rings flanking the central xylene unit. The lowest energy electronic absorption spectrum and its mirrored emission (short-axis transition dipole moments) are vibronically structured in the expected way for delocalized acene units with low excited state nuclear reorganization, with the 0–0 features determining the band maxima. For example, in Fig. 1(b) it is seen that the absorption and emission features closely match those of TIPS-Tc. The average of the 0–0 absorption and emission features indicate an S_1 energy of 2.32 eV in TIPS-BTX[60] and 2.30 eV for TIPS-Tc (Table 1). The similarity of absorption and emission features of TIPS-BTX relative to the monomer TIPS-Tc, particularly the lack of enhancement of the second vibronic component relative to the 0–0 band, is indicative of weak electronic coupling between the two chromophores of the dimer.[61] In support of this we also observe an approximate doubling of the lowest energy transition in the dimer *versus* the monomer (Fig. S1†). An absorption spectrum for TIPS-BTX was also collected in room-temperature chloroform (Fig. S2†) which has a higher energy UV cutoff than toluene. These data show the intense UV transition (peaked at 296 nm) derived from the long-axis transition dipole moment of the chromophore units. No Davydov splitting is observed, as is expected from the long bridge including two norbornyl spacers

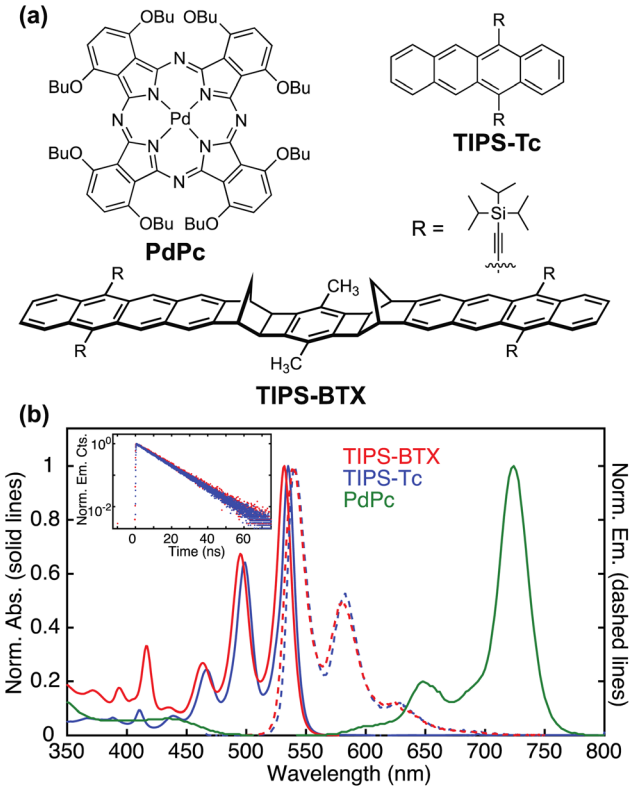

Fig. 1 (a) Chemical stick structures of annihilators TIPS-BTX & TIPS-Tc and sensitizer PdPc. (b) Room temperature absorption (solid lines) and emission (dashed lines) spectra of TIPS-BTX, TIPS-Tc and PdPc in toluene. Inset: TCSPC decay traces of TIPS-BTX & TIPS-Tc in deoxygenated 298 K toluene (λ_{ex} = 405 nm; λ_{em} = 540 nm).

as well as the near-collinear arrangement of the two chromophores of the dimer such that the higher energy transition of a split pair would be dark.

Further photophysical characterization confirms similarities between the dimer and the monomer model. The quantum yield of fluorescence for TIPS-BTX was measured to be ϕ_{FL} = 72

Table 1 Summary of relevant photophysical parameters for sensitizer and annihilators

	TIPS-Tc	TIPS-BTX	PdPc
S_1 (eV)	2.30	2.32	1.71
T_1 (eV)	1.21[a]	~1.21[b]	1.13[c]
TT (eV)	2.42[d]	<2.41[e]	—
ϕ_{FL} (%)	74	72 ± 7	—
$\tau_{0;S}$ (ns)	12.4	12.7 ± 0.5	—
$\tau_{0;T}$ (μs)	290	410	3.42

[a] Reported from a phosphorescence measurement of TIPS-Tc in a polystyrene thin film.[78] [b] It is assumed that the dimer will have a T_1 energy that is similar to TIPS-Tc (see (a)) given the nature of the chromophores. [c] Reported from a phosphorescence measurement of PdPc in toluene.[33] [d] The energy of the intermolecular multiexciton state for the monomer is approximated to be twice the T_1 energy. [e] The upper bound in this TT energy estimation relates to the T_1 yield measurement made by TA (Fig. 2) See equilibrium analysis in ESI (section S6) for details.

± 7%, comparable to that for TIPS-Tc at $\phi_{FL} = 74\%$. Regarding emissive singlet lifetimes, time-correlated single photon counting (TCSPC) measurements at 540 nm (coincident with the 0–0 transition) following excitation at 405 nm indicate mono-exponential decay for both molecules with lifetimes of $\tau_{0;S} = 12.7 \pm 0.5$ ns and $\tau_{0;S} = 12.4$ ns for TIPS-BTX and TIPS-Tc, respectively (see inset in Fig. 1(b)). Results collected at 578 nm, corresponding to the 0–1 emission transition, were consistent.

As photoluminescence measurements are insensitive to dark states that may be produced in the dynamical evolution away from the emissive state, a transient absorption (TA) experiment was performed over a time range spanning ~500 ps to 100 μs. The TA spectra obtained for TIPS-BTX (Fig. 2) are comparable to those previously reported for TIPS-Tc,[62] showing a strong ESA at ~420 nm, negative features at ~540 nm and ~580 nm, and broad weak ESA ≥ 600 nm. Of the negative features, 580 nm corresponds to stimulated emission of the 0–1 band while 540 nm is a convolution of ground state bleach and stimulated emission of the 0–0 band. The ESA with peaks at 480 nm and 520 nm and valleys at 470 nm and 490 nm comes from contributions due to bleach of the vibronically structured ground-state absorption, a quality that is also observed in TIPS-Tc and other related dimers.[62,63] These spectral features begin decaying on the order of nanoseconds with no other significant spectral evolution observed. Single wavelength kinetics traces extracted from the overall dataset exhibit decay to baseline at most wavelengths with a time scale of order 10 ns, consistent with the TCSPC measurements. However, there is minor ΔAbs persistence at long times at the 520 nm ESA maximum. The full wavelength/time dataset can be cleanly modeled using a biexponential decay function (Fig. 2), returning a major component with a lifetime of 12.9 ns (Fig. S4†) that matches well with the singlet lifetime observed *via* TCSPC (Fig. 1(b)). A long-lived component peaking at ~520 nm is also observed, but it is significantly weaker (Fig. S4†). TIPS-Tc based dimers in singlet fission studies are known to have ESA intensity in this wavelength region heralding triplet character from either triplet multiexcitonic states ($^{2S+1}$TT) or isolated triplets (T_1).[63–70] Given the long lifetime that approximately matches sensitization experiments (Fig. S6†) this weak feature observed in TIPS-BTX is best explained as arising due to formation of a small amount of isolated T_1.

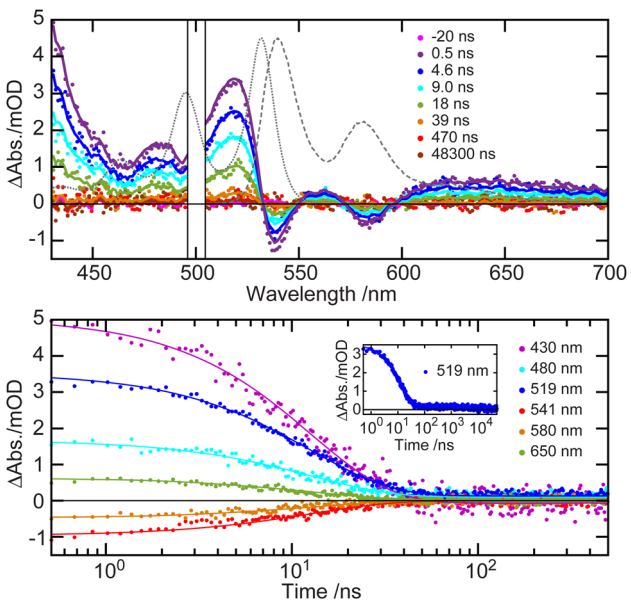

Fig. 2 (Top) Selected transient absorption spectra for TIPS-BTX in deaerated room temperature toluene as a function of time (dots are raw data; lines are from a global biexponential decay model). The region surrounding the excitation wavelength of 500 nm is removed due to pump scatter. Absorption (dotted line) and emission (dashed line) are included for reference. (Bottom) Single wavelength kinetic traces (dots) with inclusion of the biexponential model (lines). The insert is a selected kinetic trace at 519 nm to highlight the minor long-lived ESA feature.

The observation of T_1 population in such a dimer is an interesting one for fundamental reasons involving singlet fission, although we primarily address it here given its potential to complicate a comparative analysis (dimer *versus* monomer) of TTA-UC. First, we do not believe that T_1 population arises due to intersystem crossing, on the basis that no T_1 is observed in the monomer model TIPS-Tc.[62] This then raises the likelihood of an origin in singlet fission, although there is underlying complexity. In related rigid tetracenic dimers such as TIPS-BT1 [62] and TIPS-BT1′,[63] where the acene chromophores are separated by a single norbornyl bridge, we have observed formation of the multiexciton singlet ^{1}TT in equilibrium with S_1, but this equilibrated set of states decays to the ground state without observation of isolated T_1. However, other non-rigid tetracenic dimer systems have shown long-lived T_1 populations that may be presumed to originate from the multiexcitonic triplet ($^{2S+1}$TT) manifold, likely following internal conversion *via* the ^{3}TT,[56,67,69] something that is more commonly seen in pentacene-based dimers (*e.g.* ref. 71–73). We suspect that TIPS-BTX is behaving in a similar way and that the difference in its photophysics relative to the other rigid dimers TIPS-BT1 and TIPS-BT1′ has origins in its smaller isotropic spin–spin exchange interaction J due to the significantly larger bridge. Detailed studies, including time resolved EPR measurements, will be needed to fully disentangle the dynamics. A cursory estimate of T_1 yield is made for TIPS-BTX using information that includes the focal volume of the pump laser in the sample as well as a $\Delta\varepsilon$ measurement that was made for the T_1 in the related rigid dimer system TIPS-BT1′ (see ESI for details†). We find an upper bound in T_1 yield in TIPS-BTX of 6.5% and suggest that this yield is low enough to proceed with an analysis of TTA-UC that hinges upon comparisons between dimer and monomer.

As a final photophysical characterization of the annihilators, triplet lifetimes of TIPS-BTX and TIPS-Tc have been measured, as the rate constant for triplet decay is intimately tied to the probability/yield of TTA mediated by collisional interactions between excited state annihilator species. Using triplet sensitization experiments initiated by photoexcited anthracene ($\phi_{ISC} = 0.71$;[74] see ESI for details†), modest differences are uncovered between dimer and the monomer model where TIPS-BTX exhibits a triplet lifetime of $\tau_{0;T} = 410$ μs ($k_{0;T} = 2.4 \times 10^3$ s^{-1}) and where TIPS-Tc is slightly shorter at $\tau_{0;T} = 290$ μs ($k_{0;T} = 3.4$

$\times 10^3$ s^{-1})(Fig. S6†). We anticipate these lifetime differences are tied to the energy gap law where the cyclobutene/norbornyl bridge slightly raises the T_1 energy in TIPS-BTX relative to TIPS-Tc as was seen for the S_1 energies in Table 1. To put these triplet lifetime values in some context, they are long enough to expect opportunities for collision-mediated TTA, with some modest advantage expected for the dimer. However, both lifetimes remain more than an order of magnitude shorter than champion annihilator systems like DPA,[75] and several times shorter than TIPS-anthracene.[76] This general trend is understood as being due to the smaller amount of triplet energy stored in tetracenic *versus* anthracenic annihilator systems, with consequences in non-radiative excited state decay as predicted using the energy gap law. This highlights a need to identify strategies for improving TTA-UC in systems designed to process lower energy photons.

Sensitizer properties

Sensitization of TIPS-BTX and TIPS-Tc utilized the *n*-butoxide-substituted palladium phthalocyanine species shown in Fig. 1a abbreviated as PdPc, that was also previously used with another TIPS-tetracene derived rigid dimer system as mentioned in the Introduction.[33] The intersystem crossing yield ϕ_{ISC} has been reported to be 0.75 in room temperature deoxygenated benzene;[77] *i.e.* a solvent similar to the toluene used herein. Phosphorescence measurements[33] indicate the triplet stores 1.13 eV and we measure a lifetime of 3.42 μs in room temperature deoxygenated toluene (Fig. S5†). Although a unity ϕ_{ISC} is desirable, these sensitizer properties are adequate for exploration of dimer *versus* monomer trends. The electronic spectrum of PdPc is characterized by a strongly absorbing Q band observed from ~600–750 nm (see Fig. 1(b)) with minimal absorption overlap with the S_1 emission of the annihilators.

Annihilator and sensitizer together in UC systems

To explore TTA-UC property differences between dimer and monomer, a focus is placed on upconversion quantum yields (ϕ_{UC}). The expression shown in Eq. 1a is fundamentally bound at 1/2, because two absorption events are minimally required for the emission of one photon. This bounding occurs within ϕ_{TTA} (see Eq. S10†) a quantity that refers to annihilation exclusively through the singlet channel. The term f is a spin statistical factor used to account for different reactive pathways associated with singlet, triplet, and quintet character in encounter complexes between two triplets ($S = 1$ particles). It is simplified under conditions of strong exchange coupling between the two triplets such that overall spin in the encounter complex is a good quantum number (*i.e.*, $^{2S+1}(T\cdots T)$).[79] The factor f is bound at 1, a rare situation where all spin channels are without loss, for example because both $^5(T\cdots T)$ and $^3(T\cdots T)$ are unreactive and simply re-dissociate to form isolated T_1's, while the singlet encounter complex $^1(T\cdots T)$ engages in annihilation to $S_1 + S_0$.[80] If, on the other hand, $^5(T\cdots T)$ and $^3(T\cdots T)$ are fully unproductive, leading to S_0 for all species $f = \frac{1}{9}$, reflecting only the statistical weight of the singlet channel. If the $^5(T\cdots T)$ is without loss but the $^3(T\cdots T)$ decays to a single T_1 (for example due to annihilation to $T_2 + S_0$ followed by rapid internal conversion $T_2 \rightarrow T_1$) then $f = \frac{2}{5}$ (*i.e.*, 0.4) and ϕ_{UC} is bound at 20% (*i.e.*, $\frac{2}{5} \times \frac{1}{2}$). For now, we fold the f into ϕ'_{TTA} and organize initial discussions around the simpler Eq. 1b.[81] Further discussions about Eq. 1a will follow later. It is noted that when systems experience losses that are otherwise unaccounted for, the statistical factor f is the repository manifesting as a low value. This limitation of the framework is taken into account and guides the discussion later.[82]

$$\phi_{UC} = f\phi_{ISC}\phi_{TET}\phi_{TTA}\phi_{FL} \quad \text{(Eq. 1a)}$$

$$\phi_{UC} = \phi_{ISC}\phi_{TET}\phi'_{TTA}\phi_{FL} \quad \text{(Eq. 1b)}$$

$$\phi_{TET} = \frac{k_{TET}[An]}{k_{TET}[An] + k_{0;T(Sen)}} \quad \text{(Eq. 1c)}$$

$$\phi_{TTA}(\text{homofusion}) = \frac{\phi'_{TTA}}{f} = \frac{1}{2} \times \frac{2k_{TTA}[^3An^*]}{2k_{TTA}[^3An^*] + k_{0;T(An)}} = \frac{k_{TTA}[^3An^*]}{2k_{TTA}[^3An^*] + k_{0;T(An)}} \quad \text{(Eq. 1d)}$$

The outer quantities of Eq. 1b are unimolecular and depend on the yield of ISC in the sensitizer and the yield of fluorescence in the annihilator (ϕ_{ISC} and ϕ_{FL}, *vide supra*). The inner quantities on the other hand are bimolecular in nature (see typical UC schematic in Scheme 1). For the first, the yield of triplet–triplet energy transfer (ϕ_{TET}; Eq. 1c) involves photoexcited sensitizer and ground state annihilator, with dependence on the rate constant for TET (k_{TET}), on the rate constant for triplet loss in the absence of interactions with annihilator ($k_{0;T(Sen)} = 1/\tau_{0;T(Sen)}$), and on the ground state concentration of the annihilator ([An]). The second term derives from collisional interaction between a triplet excited state annihilator and another triplet. In principle this can occur either from the excited sensitizer (heterofusion) or from an excited-state annihilator species (homofusion). However, in the low relative sensitizer concentration regime that was investigated, homofusion is expected to be the dominant pathway. The simplest expression for ϕ_{TTA} under these conditions is Eq. 1d, which assumes the only loss pathways for $[^3An^*]$ population is *via* unimolecular decay of the triplet (governed by the rate constant $k_{0;T(An)}$) and bimolecular loss *via* annihilation of two $[^3An^*]$ species producing one S_1 and one S_0, governed by the rate constant k_{TTA} as well as $[^3An^*]$. As described more below, this expression can enable preliminary estimates of k_{TTA}, but there are limits to its utility under conditions where other bimolecular channels contributing to triplet loss are active.

Determination of ϕ_{TET}

Stern–Volmer studies using nanosecond TA were performed to determine ϕ_{TET} between PdPc and each of the two annihilators.

PdPc was photoexcited at 650 nm and monitored with a probe wavelength of 600 nm where the PdPc T_1 exhibits a broad excited-state absorption. Unquenched T_1 in PdPc decays to baseline monoexponentially with a fitted lifetime of $\tau_{0;T(Sen)} = 3.42$ μs (Fig. S5†), matching well with previous literature.[33,77] On the other hand, samples prepared with either TIPS-BTX or TIPS-Tc show a reduction of the PdPc T_1 lifetime that is proportional to annihilator concentration, *i.e.*, a hallmark of dynamic quenching (Fig. 3 (top)). Fitting the plotted data to the classic Stern–Volmer equation (Eq. 2) allows for the determination of the constant K_{SV}, and from this and the triplet lifetime of the sensitizer, the determination of a quenching rate constant k_q.

$$\frac{\tau_{0;T(Sen)}}{\tau_{T(Sen)}} = 1 + K_{SV}[An] = 1 + \tau_{0;T(Sen)}k_q[An] \approx 1 + \tau_{0;T(Sen)}k_{TET}[An] \quad \text{(Eq. 2)}$$

An assumption follows that Dexter energy transfer is the only operative pathway for quenching and k_q is equated with k_{TET}. From the data shown in Fig. 3 (top), a slope K_{SV} of 1026 M^{-1} and 2019 M^{-1} are determined for TIPS-BTX and TIPS-Tc, respectively, demonstrating that the monomer engages in energy transfer with the sensitizer triplet excited state more readily than the dimer, consistent with its smaller size. These slopes along with $\tau_{0;T(Sen)} = 3.42$ μs indicate $k_{TET} = 3.0 \times 10^8$ M^{-1} s^{-1} for TIPS-BTX and $k_{TET} = 5.9 \times 10^8$ M^{-1} s^{-1} for TIPS-Tc.

With these k_{TET} values in hand, the quantum yield ϕ_{TET} was calculated for all upconversion samples as [An] is varied for both monomer and dimer according to Eq. 1c. As expected from the quenching constants, TIPS-BTX at equimolar concentrations shows less efficient transfer of the triplet from the sensitizer to the annihilator as compared to TIPS-Tc (Fig. 3 (bottom)). This behavior has been seen in several previous dimeric systems[26,33,47,51] and again is explained by the larger molecular volume of dimers slowing diffusion in the solvent medium.

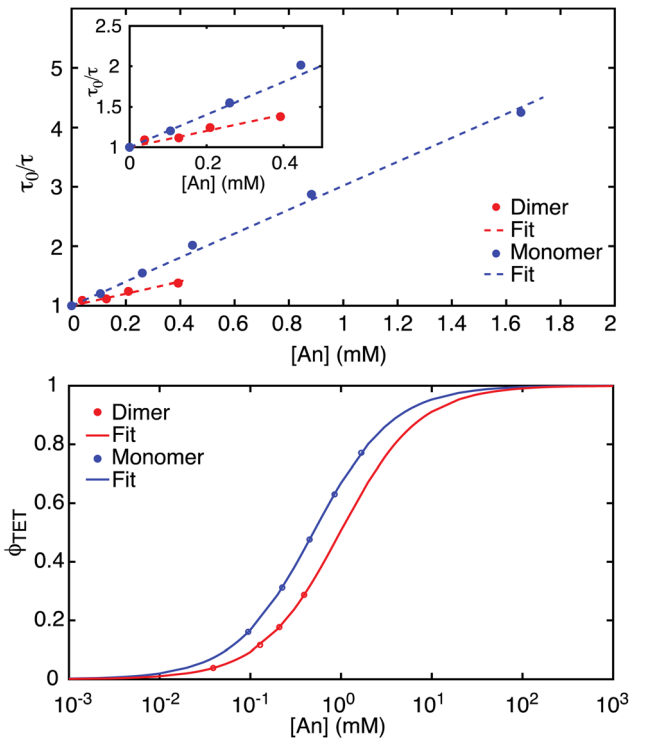

Fig. 3 (Top) Stern–Volmer plot for TIPS-BTX and TIPS-Tc in room-temperature toluene. Slopes reflecting K_{SV} along with sensitizer lifetime leads to values of $k_{TET} = 3.0 \times 10^8$ M^{-1} s^{-1} for TIPS-BTX and $k_{TET} = 5.9 \times 10^8$ M^{-1} s^{-1} for TIPS-Tc. The inset focuses on the lower annihilator concentration regime. (Bottom) Concentration dependent triplet energy transfer (TET) yields from Eq. 1c for TIPS-BTX and TIPS-Tc in room-temperature toluene.

Exploration of ϕ_{UC} and elucidation of ϕ'_{TTA} and kTTA

From the yield quantities discussed so far that depend in some way on annihilator properties (ϕ_{FL} and ϕ_{TET}), one can assume a modest advantage for the monomer TIPS-Tc over the dimer TIPS-BTX. From this perspective ϕ_{UC} is particularly interesting. Unlike for ϕ'_{TTA}, the quantification of ϕ_{UC} is experimentally straightforward using actinometry, and the value can then be used to determine ϕ'_{TTA} *via* Eq. 1b (*vide infra*). As has been discussed elsewhere,[21] there is complexity in reporting ϕ_{UC} because it is not simply dependent on the nature of the annihilator and sensitizer being used, but also on the experimental conditions of annihilator concentration [An] and photoexcitation fluence. The variable [An] influences ϕ_{TET} (Eq. 1c and Fig. 3 (bottom)) but it also impacts ϕ'_{TTA} by altering the concentration of triplets [^{3}An*] that are formed following collision with photoexcited sensitizer molecules. In a related way, photoexcitation fluence also controls [^{3}An*]. In experiments described below, both variables are explored independently in dimer *versus* monomer comparisons.

Upconversion samples of ~1.3 μM PdPc sensitizer and annihilators of varying higher concentrations were prepared in deaerated toluene (Fig. S3†) and excited with a 730 nm diode laser with fluences ranging from ~500–250 000 mW cm^{-2}. For all dimer and monomer annihilator concentrations explored, we observe the expected crossover in the upconversion emission intensity from quadratic dependence on laser fluence to linear dependence (Fig. S7–S10†). At the highest concentrations explored for TIPS-Tc, this crossover occurs at 52 W cm^{-2} (see ESI, Fig. S8 and S9† for TIPS-Tc/TIPS-BTX fluence crossover points), comparable to the crossover observed by Pun *et al.* (44.5 W cm^{-2}).[47] The crossover for TIPS-BTX is observed to be 37 W cm^{-2} at the highest concentration investigated. While still lower than the crossover observed for TIPS-Tc, we expect this would be further reduced at higher annihilator concentration where we could expect increased triplet energy transfer efficiency.[83] The crossover could be further reduced under optimal sample conditions, such as greater absorption at the excitation wavelength or when paired with an alternative sensitizer. We acknowledge that these crossing values are not insignificant, particularly when compared with those observed in anthracene system, nor expected solar fluxes. Still, this higher fluence region signals the strong annihilation regime where measurement of upconversion yield should be constant as laser fluence

increases,[84] thus allowing for independent interrogation of annihilator concentration effects (*vide infra*).

Fig. 4 (top) shows upconversion quantum yields measured *versus* laser fluence for TIPS-BTX at 0.39 mM and TIPS-Tc at 0.45 mM and at 1.67 mM. Upconversion emission spectra were corrected for self-absorption prior to integration and yields determined actinometrically against a directly excited TIPS-Tc reference in room temperature toluene (see ESI for details†). In the three cases, ϕ_{UC} saturates at higher fluences consistent with measurement in the strong annihilation regime. Critically, the dimer consistently outperforms the monomer. At comparable concentrations (0.39 mM for TIPS-BTX and 0.45 mM for TIPS-Tc) the dimer shows a maximum ϕ_{UC} (3.3%) that is more than 20 times that observed for the monomer (0.16%). But even when the monomer concentration is increased by more than a factor of three to 1.67 mM in order to affect an increase in [^{3}An*], the dimer outperforms the monomer (3.3% *versus* 0.52%; *i.e.*, a factor of 6.3 improvement).

Having established boundaries for the strong annihilation regime, a concentration-dependent study of ϕ_{UC} for dimer *versus* monomer was also made using a fixed laser fluence well into this regime at 2.3 × 10^5 mW cm^{-2} for TIPS-BTX and at 2.4 × 10^5 mW cm^{-2} for TIPS-Tc. Neither sample reaches saturation of ϕ_{UC} as a function of annihilator concentration in the range employed here, but both appear on their way, particularly in the case of the monomer where we had access to larger amounts of compound during these studies (Fig. 4 (bottom)). As was seen for excitation fluence, this plot highlights significant advantages held by the dimer *versus* the monomer. For example, at common concentrations (see the vertical dashed arrows to guide the eye), the dimer outperforms the monomer by well over an order of magnitude, even though it is worse at TET (seen in Fig. 3 (bottom)). As another example, the same UC brightness measured as ϕ_{UC} for TIPS-Tc at 1.67 mM can be achieved for TIPS-BTX at approximately an order of magnitude lower concentration (see the horizontal dashed arrow to guide the eye). At the highest fluence and concentration investigated for the dimer, a steady-state triplet concentration is calculated to be 14 μM, a factor of 27× less than the ground state concentration. This argues strongly against advantage being gained by the dimer in this diffusional setting due to a double sensitization mechanism.[26] While the maximum upconversion yield of 3.3% achieved at 0.39 mM TIPS-BTX is encouraging relative to monomer results, it does remain significantly below bluer upconverting champion systems like DPA that achieve yields ~25%.[25,26] But it is emphasized that our UC system as a whole is unoptimized, for example from the perspective of the sensitizer whose ϕ_{ISC} is 75% and whose triplet lifetime limits ϕ_{TET} at 29% at the highest annihilator concentration that was used (Fig. 3 (bottom)).

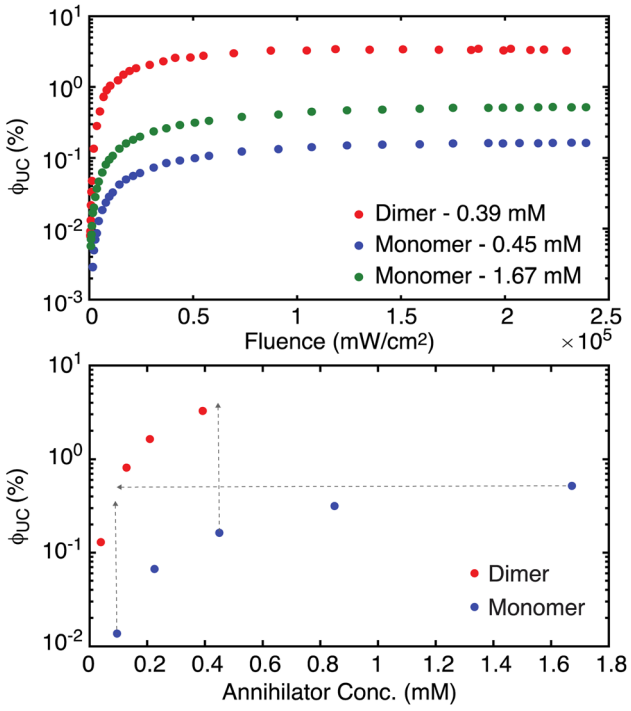

Fig. 4 (Top) Fluence dependent upconversion QY for the highest concentration dimer sample (red; 0.39 mM TIPS-BTX), a comparable concentration monomer sample (blue; 0.45 mM TIPS-Tc), and for a higher concentration monomer sample (green; 1.67 mM TIPS-Tc). Upconversion QYs asymptotically approach an upper limit as fluence increases, corresponding the transition from quadratic to linear fluence behavior. (Bottom) Upconversion QY as a function of varied annihilator concentration, measured with excitation fluence at 2.3 × 10^5 mW cm^{-2} for TIPS-BTX and 2.4 × 10^5 mW cm^{-2} for TIPS-Tc.

As was suggested at the beginning of this section, the quantification of ϕ_{UC} as a function of annihilator concentration while in the strong annihilation regime enables determination of ϕ'_{TTA} using the other known quantities in Eq. 1b. These ϕ'_{TTA} are shown in Fig. 5 and like ϕ_{UC} highlight the advantage held by the dimer but now with considerations of poorer TET from the sensitizer due to the larger dimer size removed. These data also expose the overall quality of the dimers at negotiating productive TTA. As described earlier, the theoretical limit for ϕ'_{TTA} is $\frac{1}{2}$, corresponding to a case where the spin statistical factor $f = 1$. At the larger annihilator concentrations considered here, Fig. 5

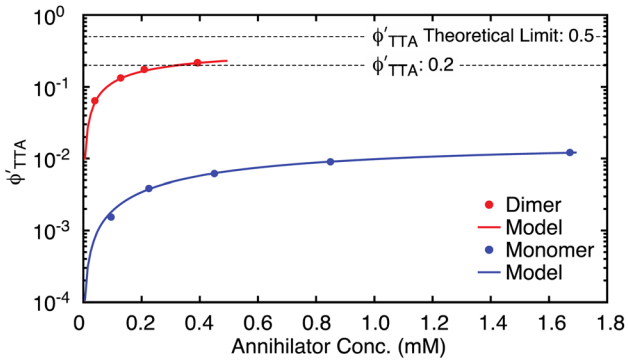

Fig. 5 ϕ'_{TTA} plotted against annihilator concentration for TIPS-Tc (blue) and TIPS-BTX (red). The results of a simplistic fitting model are included which assumes that annihilator triplet loss is only due to unimolecular decay and TTA *via* the singlet channel. See text and ESI† for discussion.

indicates that TIPS-BTX is asymptotically approaching its maximal value of ϕ'_{TTA} at the highest concentration considered (0.39 mM). The largest value that we measure is $\phi'_{TTA} = 0.21$, corresponding to $f = 0.42$ if annihilation from the singlet channel is unity. This value reflects 42% of the theoretical maximum of $\phi'_{TTA} = \frac{1}{2}$ (a case that demands $f = 1$). While smaller than what is seen in perylene-based upconversion,[80] this is on par with champion DPA systems.[25,76,85] Juxtaposed relative to the monomer at a similar concentration of 0.45 mM where $\phi'_{TTA} = 0.0062$ (corresponding to 1.2% of the theoretical maximum), this is a compelling finding. Importantly, in the limit that the other efficiencies invoked by Eq. 1b are well characterized, any additional loss pathways that detract from productive TTA would be attributed to the spin statistical factor by this analysis,[82] even when such parasitic pathways do not necessarily relate to spin statistics. In the case of TIPS-Tc presented here, we suspect a parasitic excimer state[86] (discussed in more detail later) to form from the multiexciton collision complex, leading to the low observed yield.

These ϕ'_{TTA} data can be subjected to a simple model, albeit with significant caveats alluded to below. The impetus for modeling flows from Eq. 1d which suggests that while annihilation yields are influenced by annihilator triplet lifetimes (where the dimer holds a modest advantage over the monomer (Table 1)), the rate constant k_{TTA} might in principle serve as a fundamental measure of the probability of these photophysics for a given triplet concentration. If we make the likely too-simplistic (*vide infra*) assumptions that the dimer and monomer react similarly and that the only loss pathways for annihilator triplets is from unimolecular decay and TTA *via* the singlet channel, it is possible to obtain an expression for $[^3An^*]$ as a function of annihilator concentration, with k_{TTA} as a single unknown (see Eq. S12†). This expression is then placed into Eq. 1d (or Eq. S10†), providing a fitting model for ϕ_{TTA} *versus* [An] that reveals k_{TTA}. Fig. 5 shows this modeling with the result that $k_{TTA} = 6.5 \times 10^7\ M^{-1}\ s^{-1}$ for the dimer TIPS-BTX, nearly two orders of magnitude larger than $k_{TTA} = 6.7 \times 10^5\ M^{-1}\ s^{-1}$ obtained for the monomer TIPS-Tc. It is expected that k_{TTA} is higher than stated here for the monomer, and instead TTA is in competition with parasitic second-order pathways. However, this is a behavior that is unaccounted for by a simple model, and further discussion will be focused on the apparent gains in efficiency made by the dimer TIPS-BTX.

We propose a qualitative framework towards understanding the strong variation in ϕ'_{TTA} that favors the dimer TIPS-BTX over the monomer model TIPS-Tc. This is presented in Scheme 2 which aims to highlight differences in reactive pathways available to the two systems. Both monomer and dimer start from the perspective of a collisional encounter between two triplet (T_1) excited state annihilator species (*i.e.*, relevant for homofusion). These collisional encounters are ongoing in competition with nonradiative triplet decay to ground state. The schemes for both dimer and monomer also acknowledge the underlying spin statistics where, for example, there is a 5× higher probability that the encounter complex gains quintet character compared to that of a singlet.

In the monomer system, the set of available pathways largely reflects expectations in place from studies of diffusional TTA-UC cases in the literature.[84,87] For example, the route towards S_1 emission (hν) is *via* TTA originating from a spin singlet encounter complex (summarized with the upward curved green arrow in Scheme 2 towards TTA-UC/hν). Encounter complexes with quintet character are not expected to confront loss pathways. Rather, the absence of an energetically accessible monomer-based quintet state means that re-dissociation is the most relevant outcome, forming isolated triplets that are again subjected to their own non-radiative losses.

The triplet encounter complex pathway could either dissociate in the same way just described for the quintet, or it could engage in its own reactivity such as annihilation to an energetically accessible triplet excited state followed by conversion to a single T_1 plus heat. Although general, the diagram can address why monomers such as TIPS-Tc compete poorly relative to champion systems such as DPA. The pathway 'triplet decay' is important, with the Energy Gap Law driving shorter lifetimes for the lower energy T_1 in TIPS-Tc compared to DPA. Also important and related are processes relevant to singlet fission (SF), the microscopic reverse of TTA ($S_1 \rightarrow$ multiexciton singlet $\rightarrow T_1 + T_1$). In TIPS-Tc the energy of two isolated triplets is expected to be comparable to the singlet multiexciton encounter complex or to a monomeric S_1. In other words, while singlet fission is energetically relevant in TIPS-Tc, in DPA it is uphill. As SF transiently occurs in TIPS-Tc – in particular the final step where the multiexciton singlet encounter complex dissociates (the reverse equilibrium arrow in the singlet channel) – a pair of isolated T_1 species are formed and again these are subject to their own nonradiative decay.

The reactive weight of triplet decay in this TIPS-Tc system compared to DPA means that one must work harder, in terms of excitation fluence, annihilator concentration, or both, to drive into the strong annihilation limit. However, once there, ϕ_{TTA} should not inherently be limited by smaller triplet lifetimes.[83] This then suggests other effects driven by second order interactions between excited-state annihilators. These are symbolized by the downward curved red arrows in the Scheme 2 diagram signaling non-radiative decay from the singlet or triplet encounter complexes. Here we invoke observations made by Schmidt and coworkers studying excited-state dynamics of TIPS-Tc photoexcited in high-concentration solutions.[86] These workers see evidence for singlet fission, but they also see evidence for a loss pathway *via* a spin-singlet excimer state.[87] In the context of Scheme 2 we are implying that spin-singlet or spin-triplet encounter complexes could, for certain collision geometries, encounter non-radiative loss *via* excimer channels.

For the dimer system, the key distinction relative to the TIPS-Tc monomer lies in the fact that each spin-state encounter complex ($^{1,3,5}(T\cdots T)$) has an energetically accessible internal conversion (IC) pathway where energy reapportions, leading to formation of an *intra*molecular multiexciton state ($^{1,3,5}TT$) along with one ground state dimer. In all cases this is competing against triplet dissociation. Thus, to the extent that the $^{1,3,5}TT$

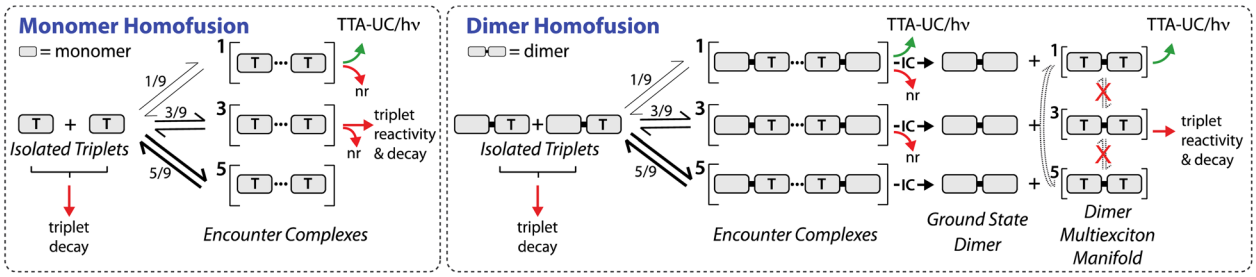

Scheme 2 Framework highlighting pathway differences available to the dimer TIPS-BTX compared to the monomer TIPS-Tc. Both systems start with an encounter complex between isolated triplets on either monomers (left) or dimers (right) and therefore the diagrams correspond to homofusion. For simplicity spin is shown as a good quantum number with spin statistics of the singlet *versus* triplet *versus* quintet channels reflected in the thickness of the equilibrium arrows. The key difference for dimers follows from internal conversion (IC) pathways. See text for further discussion.

might then access productive outcomes, IC can provide a valuable alternative to annihilator triplet decay or non-radiative loss from encounter complexes. To this last point, while TIPS-BTX has additional steric bulk relative to the monomer TIPS-Tc, its two chromophores that are juxtaposed outward remain exposed to the environment and intermolecular excimeric geometries that would be loss-inducing should remain possible. Thus, the marked improvement in ϕ_{TTA} for TIPS-BTX relative to TIPS-Tc points to the relevance of intramolecular multiexciton states.

We reason that the singlet channel is likely to be productive although we have not observed the ^{1}TT in TIPS-BTX directly (*vide supra*) and only know that the S_1 radiates efficiently ($\phi_{FL} = 0.72$) with observed decay in 12.7 ns when formed directly (Table 1). However, we can infer from a related norbornyl-bridged TIPS-pentacene dimer (TIPS-BP1′) where the ^{1}TT (storing ~1.7 eV) is formed quantitatively following visible photoexcitation. Its primary decay pathway involves non-radiative ground-state recovery in 102 ns in room temperature toluene.[63] For a system like TIPS-BTX studied here that is similarly rigid compared to TIPS-BP1′ but that stores significantly more energy in its ^{1}TT (~2.41 eV; Table 1), our expectation is that direct ^{1}TT → GS non-radiative decay will be slowed due to the energy gap law, thus affording ample time (>100 ns) for conversion to the S_1 with access to its dominant ($\phi_{FL} = 0.72$) radiative decay channel.

We also anticipate opportunities in the higher statistical weight quintet channel. Again, regarding the related TIPS-BP1′, we have recently shown using time-resolved EPR (trEPR) measurements that ^{5}TT signatures are observable,[88] a characteristic that has also been seen in other singlet fission systems including molecular dimers. This point is important because it means that the ^{1}TT (formed first from the S_1) is evolving in the multiexciton manifold to generate the ^{5}TT. By converse, and therefore relevant to this current work, an intramolecular quintet (^{5}TT) formed by IC in an upconversion system is coupled to the ^{1}TT and through it to productive photoluminescence channels (see dotted equilibrium arrows in Scheme 2). Importantly and related, the trEPR studies of TIPS-BP1′ also reveal a valuable null result: they show no evidence for evolution of the ^{5}TT into the triplet manifold, an observation that is highly unusual in the scope of SF systems that have been explored using trEPR (*e.g.* ref. 72, 73, 89 and 90). This avoidance is significant because the ^{3}TT has access to spin-allowed loss pathways (^{3}TT → T_1 + heat). Thus, if avoidance of ^{5}TT → ^{3}TT on relevant time scales is a property built into these types of rigid dimer systems, of which TIPS-BTX is a member, it would afford an opportunity to harness the higher statistical weight quintet channel towards TTA while limiting exposure to non-radiative triplet biexciton loss followed by T_1 decay. As noted in the introduction, non-rigid tetracenic dimers have been studied relative to TIPS-Tc with observation of an upconversion photoluminescence improvement of 6×[47] to 10×[56] at the highest annihilator concentrations used compared to the ~20× increase seen here (Fig. 4). It is possible that rigid tetracenic dimers are able to exploit the ^{5}TT in addition to the ^{1}TT while non-rigid systems utilize only the latter.

The last point was about protecting the ^{5}TT against loss pathways that would manifest through the triplet manifold. But this also implies that it is challenging to expect upconversion benefits in TIPS-BTX when triplet encounter complexes are initially formed, even if internal conversion to an intramolecular ^{3}TT outcompetes re-dissociation of the ^{3}(T···T) or direct non-radiative losses to T_1 *via* a triplet excimer state (*vide supra*). In TIPS-BTX, ^{3}TT → T_1 would release ~1.2 eV of heat (Table 1). While this conversion is likely slowed by Marcus inverted-region reactivity owing to expected small reorganization energy in the process (of order 200 meV),[63] it is unlikely slower than spin conversion to ^{5}TT (where it might then access the singlet manifold), a process which is governed by minor terms in the already subtle spin Hamiltonian.[88] Note that ^{1}TT → S_0 in TIPS-BP1′ is also spin allowed while releasing an even larger ~1.7 eV of heat within the Marcus inverted region. Such decay takes ~100 ns in room temperature toluene solutions.[63]

As noted earlier, Fig. 5 indicates that TIPS-BTX reaches a value of ϕ'_{TTA} that would correspond $f = 0.42$ (a lower limit achieved when ϕ_{TTA} is at its maximum of $\frac{1}{2}$), with a modest increase in f expected had higher TIPS-BTX concentrations been available. In other words, these data suggest that f is not bound at $\frac{2}{5}$ for this dimer, the scenario that would manifest if quintet encounter complexes simply dissociated while triplet encounter

complexes each decayed to a single T_1. This finding is consistent with participation by the intramolecular ^{5}TT in a productive manner for upconversion as was suggested above in the context of Scheme 2. A statistical analysis that considers the singlet and quintet channels to be entirely productive while triplet encounter complexes decay to T_1 would have $f = \frac{12}{15} = 0.8$ (see ESI for discussion†) and we anticipate this is the limit achievable by dimer systems.

Conclusion

In this work we have compared the NIR-to-visible upconversion efficacy of a new rigid dimer system TIPS-BTX relative to the monomer model TIPS-Tc, seeking to quantify differences in terms of fundamental parameters underlying upconversion yields. A key observation is that the dimer consistently and markedly outperforms the monomer. For example, at comparable concentrations (0.39 mM TIPS-BTX *versus* 0.45 mM TIPS-Tc), the dimer reaches an upconversion yield that is more than 20× larger than the monomer. When we disentangle the contribution to the yield due specifically to TTA, the dimer is found to be more than 30× more effective. To understand this, we need to look from the perspective of both types of annihilators. On one hand the monomer TIPS-Tc is highly ineffective. But the similarity of its unimolecular photophysics and single-exciton state structure compared to the dimer TIPS-BTX suggests that TIPS-Tc triplets engage in deleterious second order processes, likely from both singlet and triplet collision-complex channels. We anticipate that these involve lower-energy excimer states that steal excited state population against TTA. In the nearly co-planar dimer TIPS-BTX, the two opposing chromophores remain exposed to the environment (they are not significantly sterically crowded by the bridge), and it is difficult to imagine that excimer channels would be so significantly undermined. From this lens, the marked improvement in ϕ'_{TTA} for TIPS-BTX, to the point that it matches or exceeds what is seen in champion annihilator systems such as DPA, heralds internal conversion and subsequent participation by intramolecular multiexciton states in productive TTA. This is important, particularly under conditions where non-diffusive constructs are implemented, for example with upconversion dimers covalently decorating nanomaterial triplet sensitizers such as quantum dots. In this same context, we see the emergence of evidence that the quintet channel is productive in this rigid dimer class. First, the greater than 20× improvement in ϕ_{UC} compared to TIPS-Tc is more than 2× larger than the advantage reported for a non-rigid dimer compared to the same monomer.[47,56] This could reflect a situation where dimer rigidity prevents intramolecular ^{5}TT → ^{3}TT → T_1 loss channels while allowing for ^{5}TT → ^{1}TT → S_1 productive channels. Second, we calculate a spin-statistical value of $f = 0.42$ for TIPS-BTX with evidence that f would increase in studies with higher concentrations of the dimer. A definitive demonstration of $f > 0.4$ (*i.e.*, $\frac{2}{5}$) would be strong evidence for productive participation by ^{5}TT and this issue should continue to be explored in rigid systems. Ultimately, we posit that rigid dimers could approach $f = \frac{4}{5}$ indicating productive use of both ^{1}TT and the higher statistical weight ^{5}TT.

Data availability

Data are available upon reasonable request.

Author contributions

NHD, ATG, and RO conceived of the studies and wrote the manuscript. ATG and RO made most of the measurements. NFP collected longer-time TA data for the dimer. EGM synthesized the dimer TIPS-BTX and oversaw analyses checking against sample degradation.

Conflicts of interest

There are no conflicts to declare.

Acknowledgements

This work was funded by the National Science Foundation (CHE-2102713). RO was supported by the NSF Graduate Research Fellowship Program (NSF-GRFP; DGE 2040434). Professor Tarek Sammakia was an essential collaborator in the synthesis of TIPS-BTX (ref. 58 and 59).

Notes and references

1 T. F. Schulze and T. W. Schmidt, Photochemical upconversion: present status and prospects for its application to solar energy conversion, *Energy Environ. Sci.*, 2015, **8**, 103–125.
2 J. Zhou, Q. Liu, W. Feng, Y. Sun and F. Li, Upconversion Luminescent Materials: Advances and Applications, *Chem. Rev.*, 2015, **115**, 395–465.
3 Y. Zhou, C. Ruchlin, A. J. Robb and K. Hanson, Singlet Sensitization-Enhanced Upconversion Solar Cells via Self-Assembled Trilayers, *ACS Energy Lett.*, 2019, **4**, 1458–1463.
4 J. C. Goldschmidt and S. Fischer, Upconversion for Photovoltaics - a Review of Materials, Devices and Concepts for Performance Enhancement, *Adv. Opt. Mater.*, 2015, **3**, 510–535.
5 S. Fischer, A. Ivaturi, P. Jakob, K. W. Kramer, R. Martin-Rodriguez, A. Meijerink, B. Richards and J. C. Goldschmidt, Upconversion solar cell measurements under real sunlight, *Opt. Mater.*, 2018, **84**, 389–395.
6 T. Dilbeck and K. Hanson, Molecular Photon Upconversion Solar Cells Using Multilayer Assemblies: Progress and Prospects, *J. Phys. Chem. Lett.*, 2018, **9**, 5810–5821.
7 D. Beery, T. W. Schmidt and K. Hanson, Harnessing Sunlight via Molecular Photon Upconversion, *ACS Appl. Mater. Interfaces*, 2021, **13**, 32601–32605.
8 M. Majek, U. Faltermeier, B. Dick, R. Perez-Ruiz and A. Jacobi von Wangelin, Application of Visible-to-UV Photon

Upconversion to Photoredox Catalysis: The Activation of Aryl Bromides, *Chem.–Euro. J.*, 2015, **21**, 15496–15501.

9 B. D. Ravetz, A. B. Pun, E. M. Churchill, D. N. Congreve, T. Rovis and L. M. Campos, Photoredox catalysis using infrared light via triplet fusion upconversion, *Nature*, 2019, **565**, 343–346.

10 F. Glaser, C. Kerzig and O. S. Wenger, Sensitization-initiated electron transfer via upconversion: mechanism and photocatalytic applications, *Chem. Sci.*, 2021, **12**, 9922–9933.

11 J. C. Herrera-Luna, T. J. B. Zahringer, J. C. Herrera-Luna, M. C. Jimenez, C. Kerzig and R. Perez-Ruiz, A new green-to-blue upconversion system with efficient photoredox catalytic properties, *Phys. Chem. Chem. Phys.*, 2023, **25**, 12041–12049.

12 Q. Liu, T. Yang, W. Feng and F. Li, Blue-Emissive Upconversion Nanoparticles for Low-Power-Excited Bioimaging in Vivo, *J. Am. Chem. Soc.*, 2012, **134**, 5390–5397.

13 X. J. Zhu, Q. Q. Su, W. Feng and F. Y. Li, Anti-Stokes shift luminescent materials for bio-applications, *Chem. Soc. Rev.*, 2017, **46**, 1025–1039.

14 J. Park, M. Xu, F. Li and H.-C. Zhou, 3D Long-Range Triplet Migration in a Water-Stable Metal–Organic Framework for Upconversion-Based Ultralow-Power in Vivo Imaging, *J. Am. Chem. Soc.*, 2018, **140**, 5493–5499.

15 S. H. C. Askes and S. Bonnet, Solving the oxygen sensitivity of sensitized photon upconversion in life science applications, *Nat. Rev. Chem*, 2018, **2**, 437–452.

16 Q. Liu, M. Xu, T. Yang, B. Tian, X. Zhang and F. Li, Highly Photostable Near-IR-Excitation Upconversion Nanocapsules Based on Triplet–Triplet Annihilation for in Vivo Bioimaging Application, *ACS Appl. Mater. Interfaces*, 2018, **10**, 9883–9888.

17 S. N. Sanders, T. H. Schloemer, M. K. Gangishetty, D. Anderson, M. Seitz, A. O. Gallegos, R. C. Stokes and D. N. Congreve, Triplet fusion upconversion nanocapsules for volumetric 3D printing, *Nature*, 2022, **604**, 474.

18 J. T. Y. Wong, S. X. Wei, R. Meir, N. Sadaba, N. A. Ballinger, E. K. Harmon, X. Gao, G. Altin-Yavuzarslan, L. D. Pozzo, L. M. Campos and A. Nelson, Triplet Fusion Upconversion for Photocuring 3D-Printed Particle-Reinforced Composite Networks, *Adv. Mater.*, 2023, **35**, 2207673.

19 P. E. Keivanidis, S. Baluschev, T. Miteva, G. Nelles, U. Scherf, A. Yasuda and G. Wegner, Up-Conversion Photoluminescence in Polyfluorene Doped with Metal(II)–Octaethyl Porphyrins, *Adv. Mater.*, 2003, **15**, 2095–2098.

20 D. V. Kozlov and F. N. Castellano, Anti-Stokes delayed fluorescence from metal–organic bichromophores, *Chem. Commun.*, 2004, 2860–2861.

21 T. N. Singh-Rachford and F. N. Castellano, Photon upconversion based on sensitized triplet-triplet annihilation, *Coord. Chem. Rev.*, 2010, **254**, 2560–2573.

22 J. Zhao, S. Ji and H. Guo, Triplet–triplet annihilation based upconversion: from triplet sensitizers and triplet acceptors to upconversion quantum yields, *R. Soc. Chem. Adv.*, 2011, **1**, 937–950.

23 P. Bharmoria, H. Bildirir and K. Moth-Poulsen, Triplet–triplet annihilation based near infrared to visible molecular photon upconversion, *Chem. Soc. Rev.*, 2020, **49**, 6529–6554.

24 A. Ronchi and A. Monguzzi, Sensitized triplet–triplet annihilation based photon upconversion in full organic and hybrid multicomponent systems, *Chem. Phys. Rev.*, 2022, **3**, 041301.

25 Y. V. Aulin, M. van Sebille, M. Moes and F. C. Grozema, Photochemical upconversion in metal-based octaethyl porphyrin-diphenylanthracene systems, *R. Soc. Chem. Adv.*, 2015, **5**, 107896–107903.

26 A. Olesund, V. Gray, J. Martensson and B. Albinsson, Diphenylanthracene Dimers for Triplet-Triplet Annihilation Photon Upconversion: Mechanistic Insights for Intramolecular Pathways and the Importance of Molecular Geometry, *J. Am. Chem. Soc.*, 2021, **143**, 5745–5754.

27 J. Zhou, Z. Liu and F. Y. Li, Upconversion nanophosphors for small-animal imaging, *Chem. Soc. Rev.*, 2012, **41**, 1323–1349.

28 Q. Q. Dou, H. C. Guo and E. Y. Ye, Near-infrared upconversion nanoparticles for bio-applications, *Mater. Sci. Eng. C*, 2014, **45**, 635–643.

29 M. B. Smith and J. Michl, Singlet Fission, *Chem. Rev.*, 2010, **110**, 6891–6936.

30 V. Yakutkin, S. Aleshchenkov, S. Chernov, T. Miteva, G. Nelles, A. Cheprakov and S. Baluschev, Towards the IR Limit of the Triplet-Triplet Annihilation-Supported Up-Conversion: Tetraanthraporphyrin, *Chem.–Euro. J.*, 2008, **14**, 9846–9850.

31 Y. Y. Cheng, T. Khoury, R. G. C. R. Clady, M. J. Y. Tayebjee, N. J. Ekins-Daukes, M. J. Crossley and T. W. Schmidt, On the efficiency limit of triplet-triplet annihilation for photochemical upconversion, *Phys. Chem. Chem. Phys.*, 2010, **12**, 66–71.

32 E. Radiunas, S. Raisys, S. Jursenas, A. Jozeliunaite, T. Javorskis, U. Sinkeviciute, E. Orentas and K. Kazlauskas, Understanding the limitations of NIR-to-visible photon upconversion in phthalocyanine-sensitized rubrene systems, *J. Mater. Chem. C*, 2020, **8**, 5525–5534.

33 C. J. Imperiale, P. B. Green, E. G. Miller, N. H. Damrauer and M. W. B. Wilson, Triplet-Fusion Upconversion Using a Rigid Tetracene Homodimer, *J. Phys. Chem. Lett.*, 2019, **10**, 7463–7469.

34 M. F. Wu, D. N. Congreve, M. W. B. Wilson, J. Jean, N. Geva, M. Welborn, T. Van Voorhis, V. Bulovic, M. G. Bawendi and M. A. Baldo, Solid-State Infrared-to-Visible Upconversion Sensitized by Colloidal Nanocrystals, *Nat. Photonics*, 2016, **10**, 31–34.

35 L. Nienhaus, M. Wu, N. Geva, J. J. Shepherd, M. W. B. Wilson, V. Bulović, T. V. Voorhis, M. A. Baldo and M. G. Bawendi, Speed Limit for Triplet-Exciton Transfer in Solid-State PbS Nanocrystal-Sensitized Photon Upconversion, *ACS Nano*, 2017, **11**, 7848–7857.

36 S. Wieghold, A. S. Bieber, Z. A. VanOrman, L. Daley, M. Leger, J.-P. Correa-Baena and L. Nienhaus, Triplet Sensitization by Lead Halide Perovskite Thin Films for Efficient Solid-State Photon Upconversion at Subsolar Fluxes, *Matter*, 2019, **1**, 705–719.

37 A. Abulikemu, Y. Sakagami, C. Heck, K. Kamada, H. Sotome, H. Miyasaka, D. Kuzuhara and H. Yamada, Solid-State, Near-Infrared to Visible Photon Upconversion via Triplet-Triplet Annihilation of a Binary System Fabricated by Solution Casting, *ACS Appl. Mater. Interfaces*, 2019, **11**, 20812–20819.
38 Z. A. VanOrman and L. Nienhaus, Bulk Metal Halide Perovskites as Triplet Sensitizers: Taking Charge of Upconversion, *ACS Energy Lett.*, 2021, **6**, 3686–3694.
39 J. S. Lissau, M. Khelfallah and M. Madsen, Near-Infrared to Visible Photon Upconversion by Palladium(II) Octabutoxyphthalocyanine and Rubrene in the Solid State, *J. Phys. Chem. C*, 2021, **125**, 25643–25650.
40 C. R. Conti, A. S. Bieber, Z. A. VanOrman, G. Moller, S. Wieghold, R. D. Schaller, G. F. Strouse and L. Nienhaus, Ultrafast Triplet Generation at the Lead Halide Perovskite/Rubrene Interface, *ACS Energy Lett.*, 2022, **7**, 617–623.
41 E. Radiunas, L. Naimovicius, S. Raisys, A. Jozeliunaite, E. Orentas and K. Kazlauskas, Efficient NIR-to-vis photon upconversion in binary rubrene films deposited by simplified thermal evaporation, *J. Mater. Chem. C*, 2022, **10**, 6314–6322.
42 F. Deng, J. R. Sommer, M. Myahkostupov, K. S. Schanze and F. N. Castellano, Near-IR phosphorescent metalloporphyrin as a photochemical upconversion sensitizer, *Chem. Commun.*, 2013, **49**, 7406–7408.
43 F. Deng, W. F. Sun and F. N. Castellano, Texaphyrin sensitized near-IR-to-visible photon upconversion, *Photochem. Photobiol. Sci.*, 2014, **13**, 813–819.
44 Z. Huang, X. Li, M. Mahboub, K. M. Hanson, V. M. Nichols, H. Le, M. L. Tang and C. J. Bardeen, Hybrid Molecule–Nanocrystal Photon Upconversion Across the Visible and Near-Infrared, *Nano Lett.*, 2015, **15**, 5552–5557.
45 M. Mahboub, Z. Y. Huang and M. L. Tang, Efficient Infrared-to-Visible Upconversion with Subsolar Irradiance, *Nano Lett.*, 2016, **16**, 7169–7175.
46 Z. Huang, D. E. Simpson, M. Mahboub, X. Li and M. L. Tang, Ligand enhanced upconversion of near-infrared photons with nanocrystal light absorbers, *Chem. Sci.*, 2016, **7**, 4101–4104.
47 A. B. Pun, S. N. Sanders, M. Y. Sfeir, L. M. Campos and D. N. Congreve, Annihilator dimers enhance triplet fusion upconversion, *Chem. Sci.*, 2019, **10**, 3969–3975.
48 K. J. Fallon, E. M. Churchill, S. N. Sanders, J. Shee, J. L. Weber, R. Meir, S. Jockusch, D. R. Reichman, M. Y. Sfeir, D. N. Congreve and L. M. Campos, Molecular Engineering of Chromophores to Enable Triplet-Triplet Annihilation Upconversion, *J. Am. Chem. Soc.*, 2020, **142**, 19917–19925.
49 S. Baluschev, V. Yakutkin, T. Miteva, Y. Avlasevich, S. Chernov, S. Aleshchenkov, G. Nelles, A. Cheprakov, A. Yasuda, K. Müllen and G. Wegner, Blue-Green Up-Conversion: Noncoherent Excitation by NIR Light, *Angew. Chem., Int. Ed.*, 2007, **46**, 7693–7696.
50 D. Dzebo, K. Börjesson, V. Gray, K. Moth-Poulsen and B. Albinsson, Intramolecular Triplet–Triplet Annihilation Upconversion in 9,10-Diphenylanthracene Oligomers and Dendrimers, *J. Phys. Chem. C*, 2016, **120**, 23397–23406.
51 C. Gao, S. K. K. Prasad, B. Zhang, M. Dvořák, M. J. Y. Tayebjee, D. R. McCamey, T. W. Schmidt, T. A. Smith and W. W. H. Wong, Intramolecular Versus Intermolecular Triplet Fusion in Multichromophoric Photochemical Upconversion, *J. Phys. Chem. C*, 2019, **123**, 20181–20187.
52 H. Y. Liu, X. Y. Yan, L. Shen, Z. F. Tang, S. S. Liu and X. Y. Li, Color-tunable upconversion emission from a twisted intramolecular charge-transfer state of anthracene dimers via triplet-triplet annihilation, *Mater. Horiz.*, 2019, **6**, 990–995.
53 M. Kanoh, Y. Matsui, K. Honda, Y. Kokita, T. Ogaki, E. Ohta and H. Ikeda, Elongation of Triplet Lifetime Caused by Intramolecular Energy Hopping in Diphenylanthracene Dyads Oriented to Undergo Efficient Triplet-Triplet Annihilation Upconversion, *J. Phys. Chem. B*, 2021, **125**, 4831–4837.
54 W. J. Sun, A. Ronchi, T. H. Zhao, J. L. Han, A. Monguzzi and P. F. Duan, Highly efficient photon upconversion based on triplet-triplet annihilation from bichromophoric annihilators, *J. Mater. Chem. C*, 2021, **9**, 14201–14208.
55 F. Edhborg, H. Bildirir, P. Bharmoria, K. Moth-Poulsen and B. Albinsson, Intramolecular Triplet-Triplet Annihilation Photon Upconversion in Diffusionally Restricted Anthracene Polymer, *J. Phys. Chem. B*, 2021, **125**, 6255–6263.
56 Y. Bo, Y. Hou, D. Thiel, R. Weiss, T. Clark, M. J. Ferguson, R. R. Tykwinski and D. M. Guldi, Tetracene Dimers: A Platform for Intramolecular Down- and Up-conversion, *J. Am. Chem. Soc.*, 2023, **145**, 18260–18275.
57 S. Mattiello, S. Mecca, A. Ronchi, A. Calascibetta, G. Mattioli, F. Pallini, F. Meinardi, L. Beverina and A. Monguzzi, Diffusion-Free Intramolecular Triplet-Triplet Annihilation in Engineered Conjugated Chromophores for Sensitized Photon Upconversion, *ACS Energy Lett.*, 2022, **7**, 2435–2442.
58 E. G. Miller, M. Singh, S. R. Parkin, T. Sammakia and N. H. Damrauer, Preparation of a Rigid and nearly Coplanar Bis-Tetracene Dimer through Application of the CANAL Reaction, *ChemRxiv*, 2021, DOI: **10.26434/chemrxiv.14412200.v1**.
59 E. G. Miller, M. Singh, S. R. Parkin, T. Sammakia and N. H. Damrauer, Preparation of a Rigid and nearly Coplanar Bis-Tetracene Dimer through Application of the CANAL Reaction, *J. Org. Chem.*, 2023, **88**, 12251–12256.
60 We refer to the Frank-Condon allowed bright state as S1, while recognizing that a dark state (opposing short-axis transition dipole moments) would be lower in energy. However, Davydov splitting in this dimer is expected to be negligible given the chromophore separation. TD-DFT calculations support this, showing a < 2 meV separation between the lowest-energy dark transition to excited state 1 and the next transition that is strongly allowed to excited state 2 (see Table S4).
61 F. C. Spano, The Spectral Signatures of Frenkel Polarons in H- and J-Aggregates, *Acc. Chem. Res.*, 2010, **43**, 429–439.
62 J. D. Cook, T. J. Carey, D. H. Arias, J. C. Johnson and N. H. Damrauer, Solvent-controlled branching of localized versus delocalized singlet exciton states and equilibration

with charge transfer in a structurally well-defined tetracene dimer, *J. Phys. Chem. A*, 2017, **121**, 9229–9242.

63 A. T. Gilligan, E. G. Miller, T. Sammakia and N. H. Damrauer, Using Structurally Well-Defined Norbornyl-Bridged Acene Dimers to Map a Mechanistic Landscape for Correlated Triplet Formation in Singlet Fission, *J. Am. Chem. Soc.*, 2019, **141**, 5961–5971.

64 J. Cook, T. J. Carey and N. H. Damrauer, Solution-Phase Singlet Fission in a Structurally Well-Defined Norbornyl-Bridged Tetracene Dimer, *J. Phys. Chem. A*, 2016, **120**, 4473–4481.

65 T. Yamakado, S. Takahashi, K. Watanabe, Y. Matsumoto, A. Osuka and S. Saito, Conformational Planarization versus Singlet Fission: Distinct Excited-State Dynamics of Cyclooctatetraene-Fused Acene Dimers, *Angew. Chem., Int. Ed.*, 2018, **57**, 5438–5443.

66 S. Nakamura, H. Sakai, H. Nagashima, Y. Kobori, N. V. Tkachenko and T. Hasobe, Quantitative Sequential Photoenergy Conversion Process from Singlet Fission to Intermolecular Two-Electron Transfers Utilizing Tetracene Dimer, *ACS Energy Lett.*, 2019, **4**, 26–31.

67 Y. Matsui, S. Kawaoka, H. Nagashima, T. Nakagawa, N. Okamura, T. Ogaki, E. Ohta, S. Akimoto, A. Sato-Tomita, S. Yagi, Y. Kobori and H. Ikeda, Exergonic Intramolecular Singlet Fission of an Adamantane-Linked Tetracene Dyad via Twin Quintet Multiexcitons, *J. Phys. Chem. C*, 2019, **123**, 18813–18823.

68 A. B. Pun, A. Asadpoordarvish, E. Kumarasamy, M. J. Y. Tayebjee, D. Niesner, D. R. McCamey, S. N. Sanders, L. M. Campos and M. Y. Sfeir, Ultra-fast intramolecular singlet fission to persistent multiexcitons by molecular design, *Nat. Chem.*, 2019, **11**, 821–828.

69 K. R. Parenti, G. Y. He, S. N. Sanders, A. B. Pun, E. Kumarasamy, M. Y. Sfeir and L. M. Campos, Bridge Resonance Effects in Singlet Fission, *J. Phys. Chem. A*, 2020, **124**, 9392–9399.

70 S. Nakamura, H. Sakai, H. Nagashima, M. Fuki, K. Onishi, R. Khan, Y. Kobori, N. V. Tkachenko and T. Hasobe, Synergetic Role of Conformational Flexibility and Electronic Coupling for Quantitative Intramolecular Singlet Fission, *J. Phys. Chem. C*, 2021, **125**, 18287–18296.

71 S. N. Sanders, E. Kumarasamy, A. B. Pun, M. T. Trinh, B. Choi, J. L. Xia, E. J. Taffet, J. Z. Low, J. R. Miller, X. Roy, X. Y. Zhu, M. L. Steigerwald, M. Y. Sfeir and L. M. Campos, Quantitative Intramolecular Singlet Fission in Bipentacenes, *J. Am. Chem. Soc.*, 2015, **137**, 8965–8972.

72 M. J. Y. Tayebjee, S. N. Sanders, E. Kumarasamy, L. M. Campos, M. Y. Sfeir and D. R. McCamey, Quintet Multiexciton Dynamics in Singlet Fission, *Nat. Phys.*, 2017, **13**, 182–188.

73 H. Sakai, R. Inaya, H. Nagashima, S. Nakamura, Y. Kobori, N. V. Tkachenko and T. Hasobe, Multiexciton Dynamics Depending on Intramolecular Orientations in Pentacene Dimers: Recombination and Dissociation of Correlated Triplet Pairs, *J. Phys. Chem. Lett.*, 2018, **9**, 3354–3360.

74 M. Montalti, A. Credi, L. Prodi and M. T. Gandolfi, *Handbook of photochemistry*, CRC Press, Boca Raton FL, 3rd edn, 2006.

75 F. Edhborg, A. Olesund and B. Albinsson, Best practice in determining key photophysical parameters in triplet-triplet annihilation photon upconversion, *Photochem. Photobiol. Sci.*, 2022, **21**, 1143–1158.

76 J. K. H. Pun, J. K. Gallaher, L. Frazer, S. K. K. Prasad, C. B. Dover, R. W. MacQueen and T. W. Schmidt, TIPS-anthracene: a singlet fission or triplet fusion material?, *J. Photonics Energy*, 2018, **8**, 022006.

77 B. D. Rihter, M. E. Kenney, W. E. Ford and M. A. J. Rodgers, Synthesis and Photoproperties of Diamagnetic Octabutoxyphthalocyanines with Deep Red Optical Absorbency, *J. Am. Chem. Soc.*, 1990, **112**, 8064–8070.

78 H. L. Stern, A. J. Musser, S. Gelinas, P. Parkinson, L. M. Herz, M. J. Bruzek, J. Anthony, R. H. Friend and B. J. Walker, Identification of a Triplet Pair Intermediate in Singlet Exciton Fission in Solution, *Proc. Natl. Acad. Sci. U.S.A.*, 2015, **112**, 7656–7661.

79 D. G. Bossanyi, Y. Sasaki, S. Wang, D. Chekulaev, N. Kimizuka, N. Yanai and J. Clark, Spin Statistics for Triplet-Triplet Annihilation Upconversion: Exchange Coupling, Intermolecular Orientation, and Reverse Intersystem Crossing, *JACS Au*, 2021, **1**, 2188–2201.

80 S. Hoseinkhani, R. Tubino, F. Meinardi and A. Monguzzi, Achieving the photon up-conversion thermodynamic yield upper limit by sensitized triplet-triplet annihilation, *Phys. Chem. Chem. Phys.*, 2015, **17**, 4020–4024.

81 Y. Zhou, F. N. Castellano, T. W. Schmidt and K. Hanson, On the Quantum Yield of Photon Upconversion via Triplet-Triplet Annihilation, *ACS Energy Lett.*, 2020, **5**, 2322–2326.

82 V. Gray, A. Dreos, P. Erhart, B. Albinsson, K. Moth-Poulsen and M. Abrahamsson, Loss channels in triplet-triplet annihilation photon upconversion: importance of annihilator singlet and triplet surface shapes, *Phys. Chem. Chem. Phys.*, 2017, **19**, 10931–10939.

83 Y. Murakami and K. Kamada, Kinetics of photon upconversion by triplet–triplet annihilation: a comprehensive tutorial, *Phys. Chem. Chem. Phys.*, 2021, **23**, 18268–18282.

84 A. Haefele, J. Blumhoff, R. S. Khnayzer and F. N. Castellano, Getting to the (Square) Root of the Problem: How to Make Noncoherent Pumped Upconversion Linear, *J. Phys. Chem. Lett.*, 2012, **3**, 299–303.

85 T. W. Schmidt and F. N. Castellano, Photochemical Upconversion: The Primacy of Kinetics, *J. Phys. Chem. Lett.*, 2014, **5**, 4062–4072.

86 C. B. Dover, J. K. Gallaher, L. Frazer, P. C. Tapping, A. J. Petty, M. J. Crossley, J. E. Anthony, T. W. Kee and T. W. Schmidt, Endothermic singlet fission is hindered by excimer formation, *Nat. Chem.*, 2018, **10**, 305–310.

87 C. Ye, V. Gray, J. Martensson and K. Borjesson, Annihilation Versus Excimer Formation by the Triplet Pair in Triplet-Triplet Annihilation Photon Upconversion, *J. Am. Chem. Soc.*, 2019, **141**, 9578–9584.

88 R. D. Dill, K. E. Smyser, B. K. Rugg, N. H. Damrauer and J. D. Eaves, Entangled spin-polarized excitons from singlet fission in a rigid dimer, *Nat. Commun.*, 2023, **14**, 1180.

89 B. S. Basel, J. Zirzlmeier, C. Hetzer, S. R. Reddy, B. T. Phelan, M. D. Krzyaniak, M. K. Volland, P. B. Coto, R. M. Young, T. Clark, M. Thoss, R. R. Tykwinski, M. R. Wasielewski and D. M. Gulditla, Evidence for Charge-Transfer Mediation in the Primary Events of Singlet Fission in a Weakly Coupled Pentacene Dimer, *Chem*, 2018, **4**, 1092–1111.

90 Y. Kobori, M. Fuki, S. Nakamura and T. Hasobe, Geometries and Terahertz Motions Driving Quintet Multiexcitons and Ultimate Triplet–Triplet Dissociations via the Intramolecular Singlet Fissions, *J. Phys. Chem. B*, 2020, **124**, 9411–9419.